Rheol Acta 36:330–344 (1997)

ORIGINAL CONTRIBUTION

Gustavo A. Carri
H. Henning Winter

Mapping of the relaxation patterns of polymer melts with linear flexible molecules of uniform length

Received: 16 August 1996
Accepted: 4 March 1997

Dedicated to Prof. John D. Ferry on the occasion of his 85th birthday.

G. A. Carri
Department of Polymer Science and Engineering
University of Massachusetts
Amherst, Massachusetts 01003, USA

Prof. Dr. H. H. Winter (✉)
Department of Chemical Engineering
University of Massachusetts
Amherst, Massachusetts 01003, USA
winter@acad.umass.edu

Abstract The linear viscoelastic material functions of linear flexible polymers of uniform length are calculated from the BSW spectrum (Baumgaertel et al., 1990, 1992), and explicit analytic expressions are presented for several of the most common material functions for transient and dynamic experiments. However, numerical calculations are presented whenever needed. The BSW spectrum was determined from experimental G', G'' data of two sets of molten polymers of narrow molecular weight distribution, polystyrene and polybutadiene. The purpose of the mapping is to show a wide range of viscoelastic behavior which otherwise is not available in such comprehensive form. Experimental check of these predictions is still needed in most cases. Also, some insight into the predictions for the non-linear (including the non-equilibrium) viscoelastic behavior is achieved by studying two particular experiments: the start-up of uniaxial extension at constant rate and the start-up of shear flow at constant rate.

Key words Relaxation time spectrum – monodisperse polymers – hypergeometric function – incomplete gamma function – linear viscoelasticity – polymer dynamics

Introduction and background

John D. Ferry has pioneered the study of relations between molecular structure and linear viscoelastic properties. He has realized that a unique relaxation pattern governs (nearly) monodisperse polymers of linear flexible architecture (Ferry, 1980). One might assume that this relaxation pattern is universal since experiments on a wide range of polymers (Onogi et al., 1970; Graessley, 1974; Marin et al., 1977; Schausberger et al., 1985; Baumgaertel et al., 1992) showed that it is independent of the particular molecular structure of the polymer chain if only intermediate and long time scales are considered, i.e., for the entanglement and flow behavior. These observations are assumed to be the consequence of a universal relaxation time spectrum that depends only on a small number of material-specific parameters.

Many authors have tried to derive this universal relaxation time spectrum from first principles. The theoretical models of Rouse (1953), de Gennes (1979), Doi and Edwards (1986) and Bird et al. (1987) are able to predict the macroscopic behavior from molecular parameters and dynamics but, although they give much insight into the molecular origins of the macroscopic behavior, they fail to give good quantitative agreement with experimental data. More recent theories of des Cloizeaux (1990) and Schweizer (1995) seem to be more quantitative, but their viscoelastic predictions have not been explored enough to come to a detailed evaluation.

Experimentalists have also tried to find the functional form of this "universal" relaxation time spectrum. Among these attempts are the box-wedge shape for the spectrum proposed by Tobolsky (1960), which does not agree with experimental observations (entanglement

RA 828

"plateau" for G''), and the quite successful empirical methods of approximating the relaxation time spectrum described by Ferry (1980) to mention just a few.

While the terminal flow region has been described successfully with a stretched exponential function (Knoff et al., 1971), many of such modes are needed to include the entanglement regime. The number of parameters is large as is typical for discrete fitting functions and no physical meaning can be assigned to individual modes since they depend on the method of discretization.

Based on a detailed analysis of dynamic mechanical data of linear model polymers, Baumgaertel et al. (1990, 1992) proposed a specific form for the relaxation time spectrum (called the BSW spectrum from here on). The validity of the BSW spectrum was studied extensively elsewhere (Baumgaertel et al., 1990, 1992; Jackson et al. 1994) so we restrict ourselves to present the form of the spectrum and describe the parameters involved. The spectrum has the following form

$$H(\lambda) = \begin{cases} mG_N^0\left[\left(\frac{\lambda}{\lambda_c}\right)^{-n} + \left(\frac{\lambda}{\lambda_{\max}}\right)^{m}\right], & \text{for } \lambda \le \lambda_{\max} \\ 0, & \text{for } \lambda > \lambda_{\max} \end{cases} \tag{1a}$$

where G_N^0 is the plateau modulus, m and n are the slopes of the spectrum in the entanglement and high-frequency glass transition zones respectively, $\lambda_{\max}$ is the longest relaxation time and λ_c is the crossover time to the glass transition. The molecular weight dependence of the spectrum is implicit in the parameter $\lambda_{\max}$ defined as follows:

$$\lambda_{\max} = \lambda_c\left(\frac{M}{M_c}\right)^{z} \tag{1b}$$

Jackson et al. (1994) obtained numerical values for all these parameters for two different polymers: polystyrene and polybutadiene. These values, shown in Table 1, will be used in the present work.

Figure 1 shows the spectrum for three different polystyrene samples and three different polybutadiene samples. It can be observed that, for each polymer, the curves fall on a unique curve at short relaxation times; this agrees with the fact that in this region only short-ranged correlated motions involving a few mers are active. For long relaxation times, the spectrum vanishes, which expesses itself in a cutoff at $\lambda_{\max}$. The relaxation times are normalized with the polymer-specific crossover time, λ_c.

It is the objective of this study to explore the patterns of linear viscoelasticity of polymers with linear flexible molecules of uniform length. The classical theory of linear viscoelasticity (Ferry, 1980) interrelates the material functions. Only one material function needs to

Table 1 BSW parameters of polybutadiene at 28 °C and polystyrene at 180 °C

Parameter	Polystyrene	Polybutadiene
G_N^0 [Pa]	228000	1650000
m	0.23	0.23
n	0.67	0.73
λ_c (s)	2×10^{-4}	4.04×10^{-7}
M_c [g/mol]	16600	2714
z	3.43	3.52

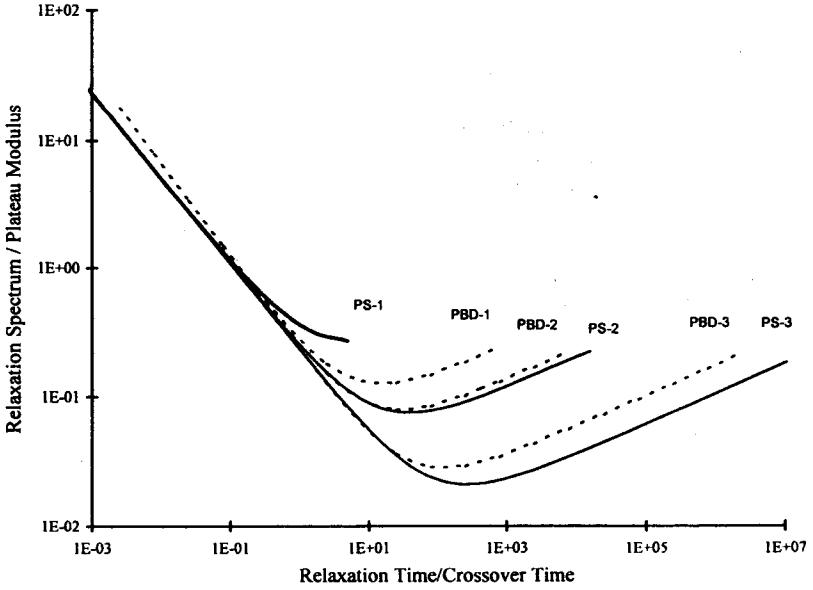

Fig. 1 BSW relaxation spectrum $H(\lambda)$ as a function of relaxation time for three polystyrene and three polybutadiene samples: PS-1 (34000 g/mol), PS-2 (292000 g/mol), PS-3 (2540000 g/mol), PBD-1 (18100 g/mol), PBD-2 (37900 g/mol) and PBD-3 (201000 g/mol). Parameters are given in Table 1

be known, which in our case is the BSW spectrum (as a nearly perfect reproduction of G', G'' data). The use of the BSW spectrum is advantageous because of two reasons: first, it provides analytical expressions for the material functions which are quantitative (as G', G'' data would yield) and, second, it reduces the description of the linear viscoelastic behavior of any polymer melt with very narrow molecular weight distribution to the determination of only five material-specific parameters. The resulting pattern is expected to be universally valid in the linear region. Non-linear predictions with the BWS spectrum are not universal since they involve specific choices of constitutive equations. This will be explored in two examples in order to demonstrate deviations from linearity. The entire study focuses on the flow and entanglement regions of molten polymers. The glass behavior at short times is not included in this study.

BSW predictions

The universality of the relaxation time spectrum expresses itself in a universal set of linear viscoelastic material functions which, in their universality, have hardly been explored. The most important ones of these material functions will be mapped out by introducing the BSW spectrum (Eq. (1)) into Boltzmann's classical equation of linear viscoelasticity for the stress

$$\tau(t) = \int_{-\infty}^{t} dt' 2\boldsymbol{D}(t') \int_{0}^{\lambda_{max}} \frac{d\lambda}{\lambda} H(\lambda) e^{-\frac{(t-t')}{\lambda}} \tag{2}$$

$2\boldsymbol{D}(t')$ is the rate of strain tensor.

The BSW retardation time spectrum

The relaxation time spectrum is not the only type of spectrum that is capable of describing the linear viscoelastic behavior (Ferry, 1980). An alternative is the retardation time spectrum, $L(\lambda)$, which, in particular, is more convenient for calculating the creep compliance as will be shown further below. For fluids, the two types of spectra are related by the following expression (Gross, 1953)

$$H(\lambda)L(\lambda) = \left\{ \left[\frac{1}{H(\lambda)} \int_{-\infty}^{\infty} \mathrm{d}\ln(u) \frac{H(u)}{\frac{\lambda}{u} - 1} \right]^2 + \pi^2 \right\}^{-1} \tag{3}$$

The integral in the denominator cannot be calculated in general, but the particular case of the BSW spectrum has an analytical solution. The primitive is expressed in terms of generalized hypergeometric functions (Gradshteyn, 1980). For example, if only the entanglement part of the spectrum, $H_e = mG_N^0(\lambda/\lambda_{max})^m$, is used (the calculation for the glassy part is similar), the primitive is the following

$$\int_{-\infty}^{\infty} \frac{H_e(u)}{\frac{\lambda}{u} - 1} \mathrm{d}\ln(u) = mG_N^0 \pi \left\{ \mathrm{ctg}(m\pi) \left(\frac{\lambda}{\lambda_{max}} \right)^m - \frac{1}{\pi m} F\left(1, -m; 1-m; \frac{\lambda}{\lambda_{max}} \right) \right\} \tag{4}$$

where F is the hypergeometric function (see Appendix A). Using this result and the similar one obtained for the glassy part of the spectrum, the analytic expression of the BSW retardation time spectrum is the following.

$$L(\lambda) = \left[\left\{ \left(\frac{\lambda_c}{\lambda_{max}} \right)^n \left[\frac{1}{n\pi} F\left(1, n; 1+n; \frac{\lambda}{\lambda_{max}} \right) - \mathrm{ctg}(n\pi) \left(\frac{\lambda}{\lambda_{max}} \right)^{-n} \right] + \left[\mathrm{ctg}(m\pi) \left(\frac{\lambda}{\lambda_{max}} \right)^m - \frac{1}{m\pi} F\left(1, -m; 1-m; \frac{\lambda}{\lambda_{max}} \right) \right] \right\}^2 + \left[\left(\frac{\lambda}{\lambda_c} \right)^{-n} + \left(\frac{\lambda}{\lambda_{max}} \right)^m \right]^2 \right]^{-1} \left[\left(\frac{\lambda}{\lambda_c} \right)^{-n} + \left(\frac{\lambda}{\lambda_{max}} \right)^m \right] \frac{1}{mG_N^0 \pi^2} \tag{5a}$$

In the case of retardation times shorter than the crossover time ($\lambda < \lambda_c$), this spectrum can be approximated by the following expression.

$$L(\lambda) = \frac{1}{mG_N^0 \pi^2 \sin^2(n\pi)} \left(\frac{\lambda}{\lambda_c} \right)^n. \tag{5b}$$

Figure 2 shows the BSW retardation time spectra for the same polystyrene and polybutadiene samples studied before. Again, for each polymer, the curves fall on a unique curve at short retardation times as in the case of the relaxation spectra. The values of the slope, n, for polystyrene and polybutadiene are 0.679 and 0.74, respectively. Finally, when the retardation time approaches λ_{max}, the hypergeometric functions go to infinity, thus the BSW retardation spectrum approaches zero very quickly. The maximum retardation time is equal to the longest relaxation time, λ_{max}. It is important to mention the very good qualitative agreement between our prediction and the experimental results obtained for nearly monodisperse poly(cis-isoprene) by Nemoto and coworkers (Nemoto et al., 1972).

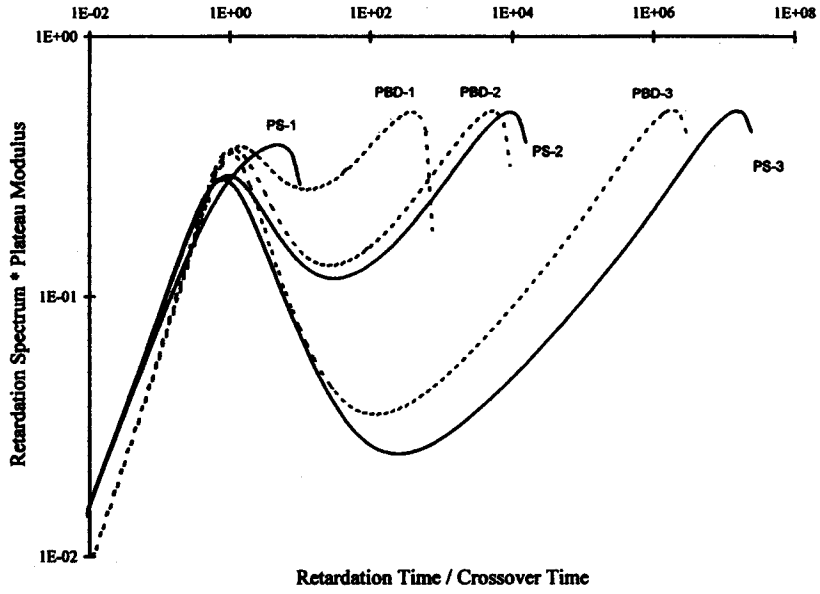

Fig. 2 BSW retardation spectrum as a function of retardation time for three polystyrene and three polybutadiene samples: PS-1 (34000 g/mol), PS-2 (292000 g/mol), PS-3 (2540000 g/mol), PBD-1 (18100 g/mol), PBD-2 (37900 g/mol) and PBD-3 (201000 g/mol)

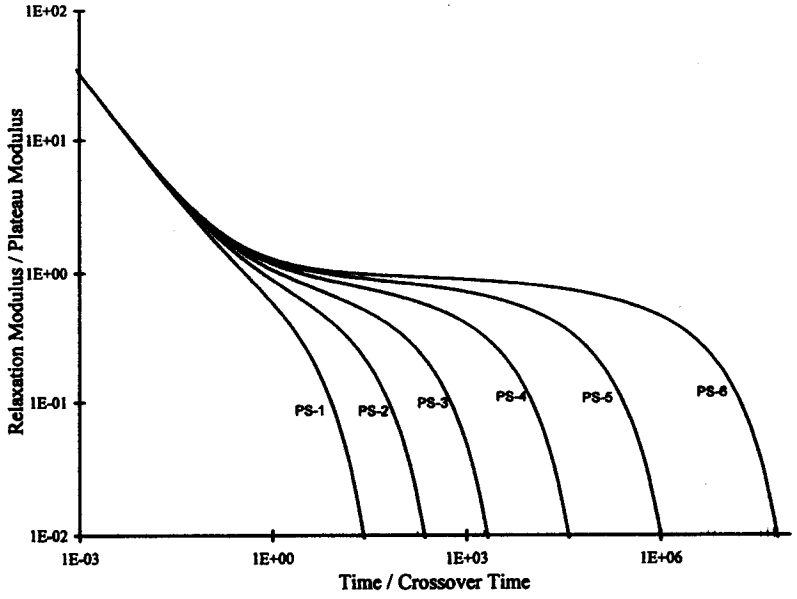

Fig. 3 Relaxation modulus as a function of time for six polystyrene samples: PS-1 (34000 g/mol), PS-2 (65000 g/mol), PS-3 (125000 g/mol), PS-4 (292000 g/mol), PS-5 (757000 g/mol) and PS-6 (2540000 g/mol)

The relaxation modulus

One of the most frequently used material functions is the relaxation modulus which gives a measure of the stiffness of the material. The relation between this quantity and the relaxation time spectrum is given by the following equation:

$$G(t) = \int_0^\infty \frac{d\lambda}{\lambda} H(\lambda) e^{-\frac{t}{\lambda}}. \tag{6}$$

It is of interest to study the relaxation modulus predicted by the BSW spectrum. $H(\lambda)$ is given by Eq. (1) and the upper limit of the integral is λ_{max}. The resulting relaxation modulus is a linear superposition of two incomplete gamma functions (see Appendix B).

$$G(t) = mG_N^0 \left(\frac{t}{\lambda_{max}}\right)^m \Gamma\left(-m, \frac{t}{\lambda_{max}}\right) + mG_N^0 \left(\frac{\lambda_c}{t}\right)^n \Gamma\left(n, \frac{t}{\lambda_{max}}\right) \tag{7}$$

Figure 3 shows this relaxation modulus for six polystyrene samples. The glass transition, entanglement and flow regions can be seen clearly. Also, a unique curve, independent of molecular weight, can be seen at short

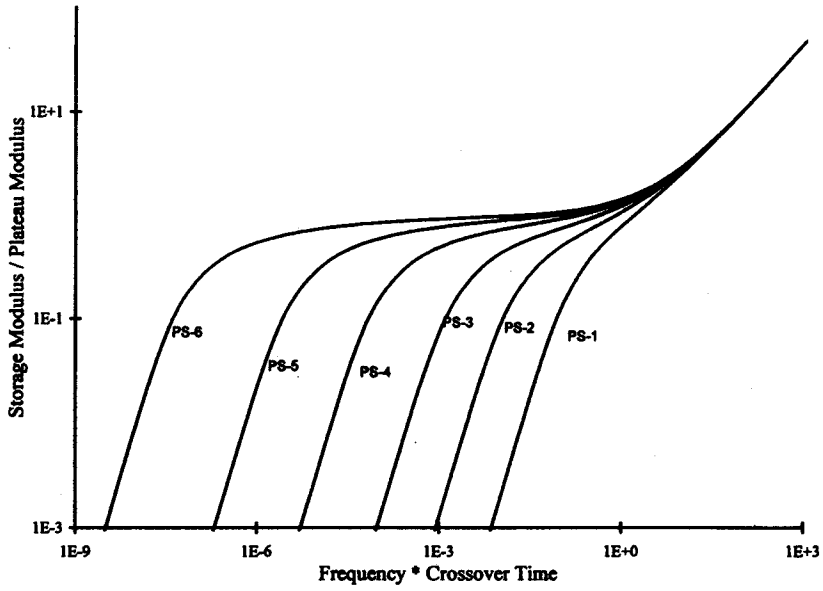

Fig. 4 Storage modulus as a function of frequency for six polystyrene samples: PS-1 (34000 g/mol), PS-2 (65000 g/mol), PS-3 (125000 g/mol), PS-4 (292000 g/mol), PS-5 (757000 g/mol) and PS-6 (2540000 g/mol)

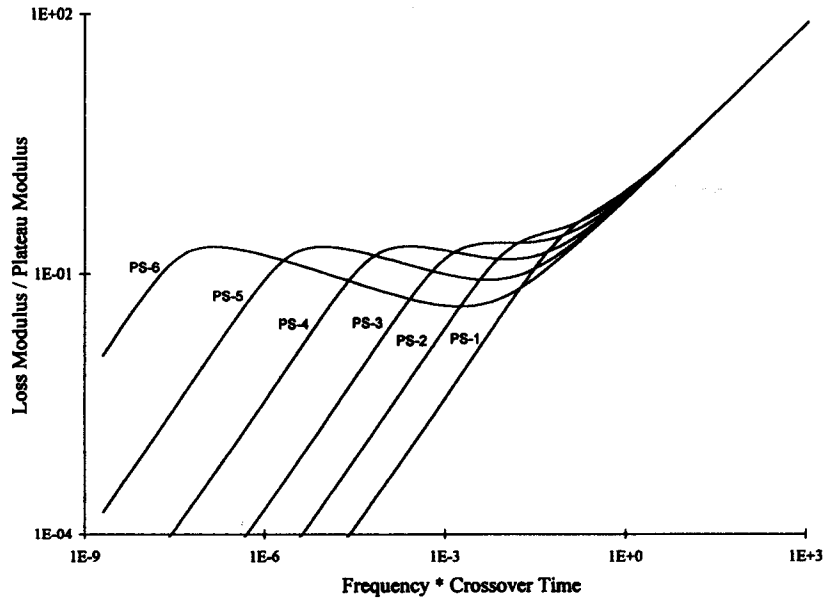

Fig. 5 Loss modulus as a function of frequency for six polystyrene samples: PS-1 (34000 g/mol), PS-2 (65000 g/mol), PS-3 (125000 g/mol), PS-4 (292000 g/mol), PS-5 (757000 g/mol) and PS-6 (2540000 g/mol)

times. The length of the rubbery plateau increases as the molecular weight increases (increasing λ_{max}/λ_c). Similar results were obtained for seven polybutadiene samples.

Dynamic mechanical behavior

The dynamic mechanical modulus is one of the most sensitive and informative material functions for polymeric systems. Relaxation processes appear as peaks in the loss modulus allowing us to determine the temperature at which a particular relaxation mode is activated and, therefore, giving a quantitative measure of the activation energy for particular modes such as the glass transition (alpha relaxation), the beta relaxation, and others. As a consequence of this, it is of interest to see if the dynamic quantities predicted by the BSW spectrum reproduce the experimental data. Although this calculation has been done previously numerically (Baumgaertel et al., 1990, 1992), the purpose is to get an analytical expression for the storage and loss moduli. It is clear that only the dynamic modulus or the dynamic compliance is required because of their interrelation (Ferry, 1980):

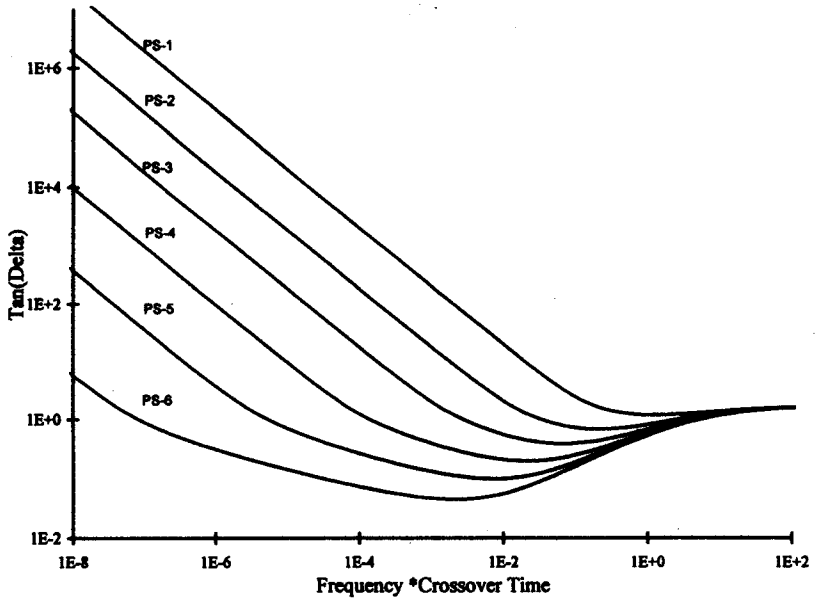

Fig. 6 Tan (δ) as a function of frequency for six polystyrene samples: PS-1 (34000 g/mol), PS-2 (65000 g/mol), PS-3 (125000 g/mol), PS-4 (292000 g/mol), PS-5 (757000 g/mol) and PS-6 (2540000 g/mol)

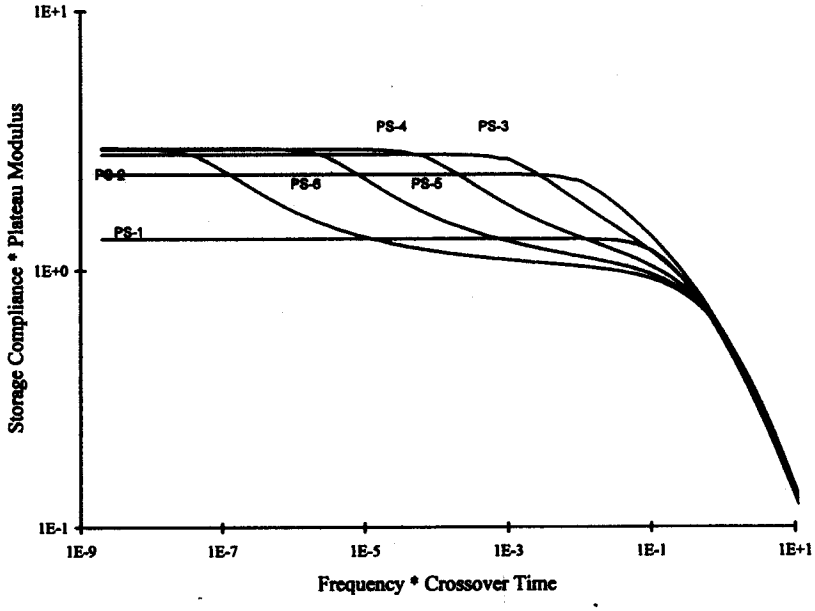

Fig. 7 Storage compliance as a function of frequency for six polystyrene samples: PS-1 (34000 g/mol), PS-2 (65000 g/mol), PS-3 (125000 g/mol), PS-4 (292000 g/mol), PS-5 (757000 g/mol) and PS-6 (2540000 g/mol)

$$G^*J^* = 1 \tag{8}$$

The storage modulus and the loss modulus depend on the relaxation spectrum by (Ferry, 1980)

$$G'(\omega) = \int_0^\infty \frac{d\lambda}{\lambda} H(\lambda) \frac{(\omega\lambda)^2}{1+(\omega\lambda)^2}$$

$$G''(\omega) = \int_0^\infty \frac{d\lambda}{\lambda} H(\lambda) \frac{(\omega\lambda)}{1+(\omega\lambda)^2}. \tag{9}$$

In the particular case of the BSW spectrum, these integrals can be solved analytically.

$$G'(\omega) = mG_N^0(\omega\lambda_{\max})^2 \left\{ \left(\frac{\lambda_c}{\lambda_{\max}}\right)^n \frac{1}{2-n} F\left(1, 1-\frac{n}{2}; 2-\frac{n}{2}; -(\omega\lambda_{\max})^2\right) + \frac{1}{2+m} F\left(1, 1+\frac{m}{2}; 2+\frac{m}{2}; -(\omega\lambda_{\max})^2\right) \right\} \tag{10}$$

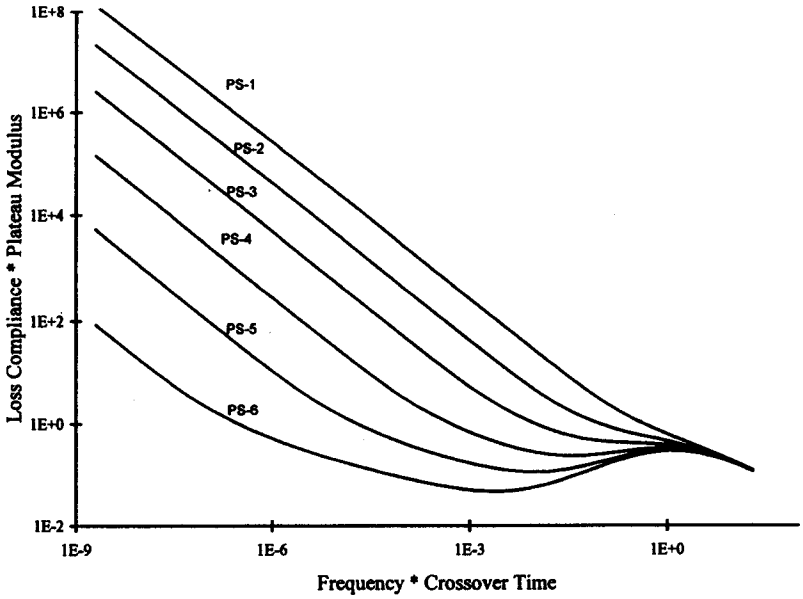

Fig. 8 Loss compliance as a function of frequency for six polystyrene samples: PS-1 (34000 g/mol), PS-2 (65000 g/mol), PS-3 (125000 g/mol), PS-4 (292000 g/mol), PS-5 (757000 g/mol) and PS-6 /2540000 g/mol)

$$G''(\omega) = G_N^0 m\omega\lambda_{\max}\left\{\left(\frac{\lambda_c}{\lambda_{\max}}\right)^n \frac{1}{1-n} F\left(1, \frac{1-n}{2}; \frac{3-n}{2}; -(\omega\lambda_{\max})^2\right) + \frac{1}{1+m} F\left(1, \frac{1+m}{2}; \frac{3+m}{2}; -(\omega\lambda_{\max})^2\right)\right\} \tag{11}$$

where F is the generalized hypergeometric function.

Figures 4 to 8 show the different dynamic quantities for the six polystyrene samples. At high frequencies all these curves merge into a unique curve, independent of molecular weight. The mapping of Figs. 4 and 5 onto the experimental data is within experimental error as was shown by Baumgaertel et al. (1990, 1992) and Jackson et al. (1994). Similar results were obtained for seven polybutadiene samples.

The creep compliance

The creep compliance has been calculated mostly in the following three different ways. First, if the storage or loss compliance is known, a simple Fourier Transform gives us the desired result. In our case, the expression for the dynamic compliance is so complicated that the integration cannot be done analytically. The second approach is to calculate the creep compliance from the retardation spectrum. Again, the complicated expression cannot be integrated analytically. The third approach is to calculate the Laplace transform of the creep compliance and then try to invert it. In this case, although the Laplace transform can be obtained analytically, the inverse is not available. Therefore, the creep compliance was calculated numerically using the second approach.

$$J(t) = \int_0^\infty \frac{d\lambda}{\lambda} L(\lambda)(1 - e^{-\frac{t}{\lambda}}) + \frac{t}{\eta_0} \tag{12}$$

The integral was discretized with the trapezoids method. In support of these calculations very good numerical agreement between the recoverable compliance calculated numerically and analytically was observed.

The results for the six polystyrene samples are shown in Fig. 9. The plot shows a unique behavior, independent of molecular weight, at short times and a plateau region that increases with increasing molecular weight. The predicted behavior compares well with published experimental observations as reported by Ferry (1980). Similar patterns were observed with seven polybutadiene samples.

Steady shear properties of the BSW spectrum

Among the most common viscoelastic properties in steady shear experiments are: the zero-shear viscosity η_0, the first normal stress function ψ_1 and the recoverable compliance J_e^0. The BSW spectrum allows analytic expressions to be calculated for all these material functions:

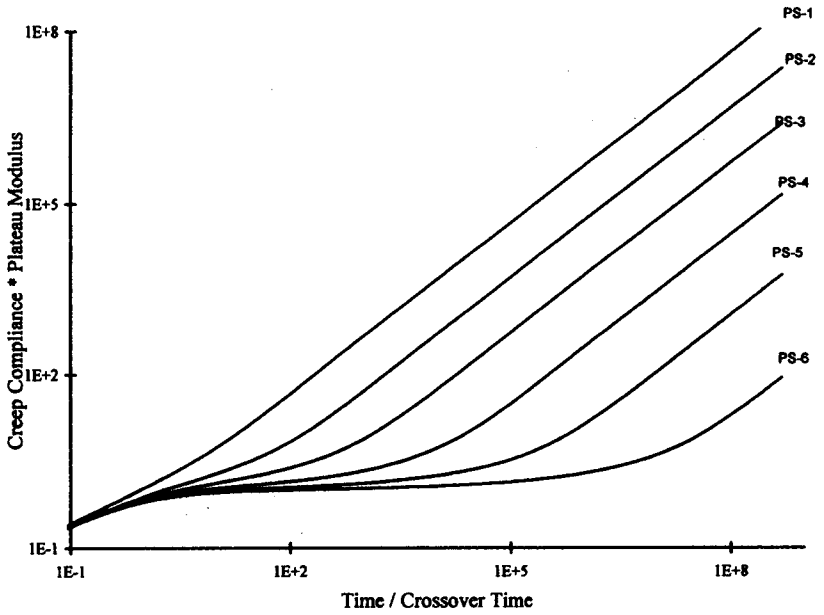

Fig. 9 Creep compliance as a function of time for six polystyrene samples: PS-1 (34000 g/mol), PS-2 (65000 g/mol), PS-3 (125000 g/mol), PS-4 (292000 g/mol), PS-5 (757000 g/mol) and PS-6 (2540000 g/mol)

Table 2 Steady shear properties

Sample	M_W [g/mol]	λ_{max} (s)	η_0 [Pa s]	ψ_1 [Pa s^2]	J_e^0 [1/Pa]
Polystyrene	34000	2.34×10^{-3}	171.3	0.34	5.80×10^{-6}
Polystyrene	65000	2.16×10^{-2}	1069	23.53	1.03×10^{-5}
Polystyrene	125000	2.03×10^{-1}	8986	1978	1.22×10^{-5}
Polystyrene	292000	3.73×10^{0}	1.60×10^{5}	6.58×10^{5}	1.28×10^{-5}
Polystyrene	757000	9.80×10^{1}	4.18×10^{6}	4.52×10^{8}	1.29×10^{-5}
Polystyrene	2540000	6.23×10^{3}	2.66×10^{8}	1.83×10^{12}	1.29×10^{-5}
Polybutadiene	18100	3.21×10^{-4}	1.03×10^{2}	3.56×10^{-2}	1.69×10^{-6}
Polybutadiene	20700	5.16×10^{-4}	1.63×10^{2}	9.13×10^{-2}	1.72×10^{-6}
Polybutadiene	37900	4.33×10^{-3}	1.34×10^{3}	6.41×10^{0}	1.77×10^{-6}
Polybutadiene	44100	7.39×10^{-3}	2.29×10^{3}	1.86×10^{1}	1.78×10^{-6}
Polybutadiene	70200	3.79×10^{-2}	1.17×10^{4}	4.90×10^{2}	1.78×10^{-6}
Polybutadiene	97000	1.18×10^{-1}	3.66×10^{4}	4.78×10^{3}	1.79×10^{-6}
Polybutadiene	201000	1.54×10^{0}	4.75×10^{5}	8.06×10^{5}	1.79×10^{-6}

$$\eta_0 = \int_0^{\lambda_{max}} H(\lambda)d\lambda = \frac{m}{1+m} G_N^0 \lambda_{max} \left\{1 + \frac{1+m}{1-n}\left(\frac{M_c}{M}\right)^{nz}\right\} \quad (13)$$

$$\psi_1 = 2\int_0^{\lambda_{max}} \lambda H(\lambda)d\lambda = \frac{2m}{2+m} G_N^0 \lambda_{max}^2 \left\{1 + \frac{2+m}{2-n}\left(\frac{M_c}{M}\right)^{nz}\right\} \quad (14)$$

$$J_e^0 = \frac{(1+m)^2\left\{1 + \frac{2+m}{2-n}\left(\frac{M_c}{M}\right)^{nz}\right\}}{m(2+m)G_N^0\left\{1 + \frac{1+m}{1-n}\left(\frac{M_c}{M}\right)^{nz}\right\}^2} \quad (15)$$

where M is the molecular weight of the sample and M_c is the crossover molecular weight. Table 2 shows the value of these viscoelastic quantities for each of the samples. The contribution of the glass transition is included here (expressions in wavy brackets) but it can be considered negligible for high molecular weights, $M \gg M_c$.

The start-up of uniaxial extension at constant rate

The BSW spectrum might also be useful for predicting non-linear behavior during the start-up of uniaxial extension at constant rate. This experiment has been analyzed previously by Chang et al. (1972) to explain Meissner's experimental observations (Meissner, 1971) but using a different relaxation spectrum (for broadly distributed polymers).

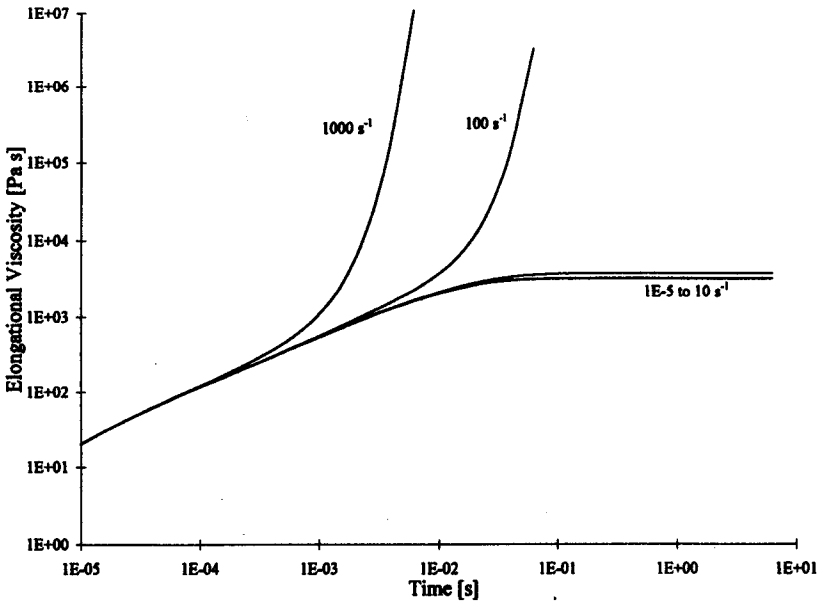

Fig. 10 Elongational viscosity, $(\tau_{11} - \tau_{22})/\dot{\varepsilon}_0$, as a function of time for a polystyrene sample with a molecular weight of 65000 g/mol. The different shear rates are shown

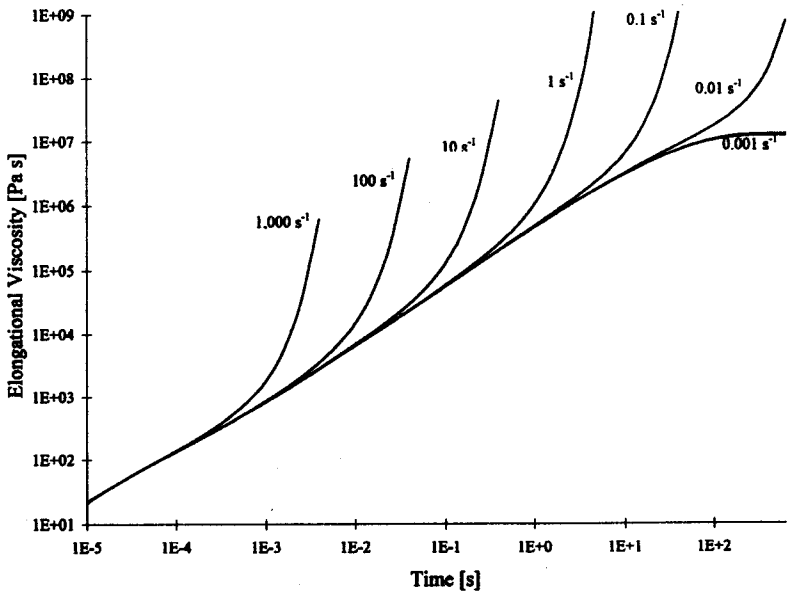

Fig. 11 Elongational viscosity, $(\tau_{11} - \tau_{22})/\dot{\varepsilon}_0$, as a function of time for a polystyrene sample with a molecular weight of 757000 g/mol. The different shear rates are shown

To study the predictions of the BSW spectrum, we chose the single integral constitutive equation of Lodge (1964).

$$\tau(t) = \int_{-\infty}^{t} dt' m_f(t;t') C^{-1}(t;t') \tag{16}$$

Among all the possible strain tensors available, we have chosen Finger's strain tensor $C^{-1}(t;t')$. The memory function is expressed in terms of the relaxation spectrum by

$$m_f(t-t') = -\frac{dG(t-t')}{d(t-t')} = \int_0^{\lambda_{max}} d\lambda \frac{H(\lambda)}{\lambda^2} e^{-\frac{(t-t')}{\lambda}} \tag{17}$$

We consider a polymer which is fully equilibrated until, at time $t=0$, it gets stretched at constant rate $\dot{\varepsilon}_0$. The relative length change of the sample is prescribed as

$$\frac{l(t)}{l(0)} = e^{\varepsilon(t)} = \begin{cases} e^{\dot{\varepsilon}_0 t} & -\infty < t' < 0 \\ e^{\dot{\varepsilon}_0 (t-t')} & 0 < t' < t \end{cases} \tag{18}$$

Thus, using Finger's strain tensor and the previous expression for the memory function, the stress response can be written in component form.

$$\tau_{11}-\tau_{22}=\int_0^{\lambda_{max}} d\lambda \frac{H(\lambda)}{\lambda}\left\{\frac{1-2\dot{\varepsilon}_0\lambda e^{-(1-2\dot{\varepsilon}_0\lambda)\frac{t}{\lambda}}}{1-2\dot{\varepsilon}_0\lambda}-\frac{1+\dot{\varepsilon}_0\lambda e^{-(1+\dot{\varepsilon}_0\lambda)\frac{t}{\lambda}}}{1+\dot{\varepsilon}_0\lambda}\right\} \tag{19}$$

In our case, the relaxation time spectrum is prescribed for monodisperse polymers (Eq. (1)). Figures 10 and 11 show the elongational viscosity, $(\tau_{11}-\tau_{22})/\dot{\varepsilon}_0$, for two polystyrene samples with molecular weights 65000 and 757000 g/mol, respectively. The qualitative behavior is the one observed previously by Chang. Figure 10 shows that the viscosity diverges to infinity if the stretching rate is larger than $10\ s^{-1}$ and the divergence begins at times close to the inverse of the stretching rate. If the stretching rate is below or equal to $10\ s^{-1}$, the viscosity reaches a limiting value. In Fig. 11 a similar behavior can be observed. Again, the viscosity diverges to infinity if the stretching rate is larger than $0.001\ s^{-1}$ and the divergence begins at times approximately equal to the inverse of the stretching rate. Also, if the stretching rate is below or equal to $0.001\ s^{-1}$, the viscosity reaches a limiting value at long times.

It is interesting to observe that the value of the elongational viscosity at short times is independent of molecular weight. Figures 10 and 11 show this result very clearly. This is a direct consequence of the model and will be discussed later.

Finally, the plots show some curvature at short times. This is not an inaccuracy of the calculation which is accurate up to the fifth significant digit. Therefore, it should be taken as a prediction of the model.

The start-up of shear flow at constant rate – Viscoelasticity of the non-equilibrium state

A sample is held at rest until it is fully equilibrated. Then, at time $t=0$, shear flow is imposed at constant rate $\dot{\gamma}$. The shear stress response is calculated using the single integral constitutive equation of Lodge (1964) but, since the viscoelasticity of a non-equilibrium state is to be described, a damping function must be included in the calculations (Wagner, 1976). As before, we have chosen Finger's strain tensor as the strain measure and the memory function has been expressed in terms of the relaxation spectrum (Eq. (17)). Among all the available damping functions (Wagner, 1976, 1978; Osaki, 1976; Laun, 1978; Papanastasiou et al., 1983; Soskey et al., 1984), we have chosen Wagner's expression for this function because it requires only one parameter and its functional form is easy to deal with. The explicit form of the damping function

$$h(t;t')=e^{-n_1\gamma(t;t')} \tag{20}$$

depends on the shear strain

$$\gamma(t;t')=\int_{t'}^{t} dt''\dot{\gamma}(t'') \tag{21}$$

where the parameter "n_1" is not known for our samples. Generally, the numerical value of this parameter is between 0.2 and 0.3 so we take a value of 0.25 for our analysis. The arbitrary selection of this parameter invalidates the quantitative predictions of our calculation, but allows us to study the predictions of the BSW spectrum qualitatively. In particular, we want to investigate how the BSW spectrum, together with h, predict shear thinning and stress overshoot.

The shear stress as described with the above equation

$$\tau_{12}=\tau_{21}=\int_{-\infty}^{t} dt' m_f(t-t')h(t;t')\gamma(t;t') \tag{22}$$

needs to be evaluated for the strain history

$$\gamma(t;t')=\begin{cases}\dot{\gamma}_0 t & -\infty<t'<0\\ \dot{\gamma}_0(t-t') & 0<t'<t\end{cases} \tag{23}$$

After substitution of Eqs. (17, 20, 21, 23) into Eq. (22), the shear stress can be written in the following form

$$\tau_{12}(t,\dot{\gamma}_0)=\dot{\gamma}_0\int_0^{\lambda_{max}} d\lambda H(\lambda)\left[\left\{\frac{tn_1\dot{\gamma}_0}{(1+n_1\dot{\gamma}_0\lambda)}-\frac{1}{(1+n_1\dot{\gamma}_0\lambda)^2}\right\}e^{-\frac{t(1+n_1\dot{\gamma}_0\lambda)}{\lambda}}+\frac{1}{(1+n_1\dot{\gamma}_0\lambda)^2}\right] \tag{24}$$

The integral in Eq. (24), together with Eq. (1) for $H(\lambda)$, needs to be evaluated numerically. Figures 12 and 13 show the resulting shear viscosity for two polystyrene samples with molecular weights of 65000 and 757000 g/mol, respectively. The stress overshoot can be seen in both plots clearly. In the first case, molecular weight of 65000 g/mol, the maximum relaxation time is 0.0216 s, while in the second case, molecular weight of 757000 g/mol, it is 98 s. In both cases, the stress overshoot is observed for shear rates larger than $1/\lambda_{max}$ and the stress maxima occur at shear strain, $\dot{\gamma}t$, values which are equal to the inverse of the damping parameter, n_1. It is of importance to mention the fact that the shear viscosity at very short times is independent of molecular weight which is shown in both figures. This

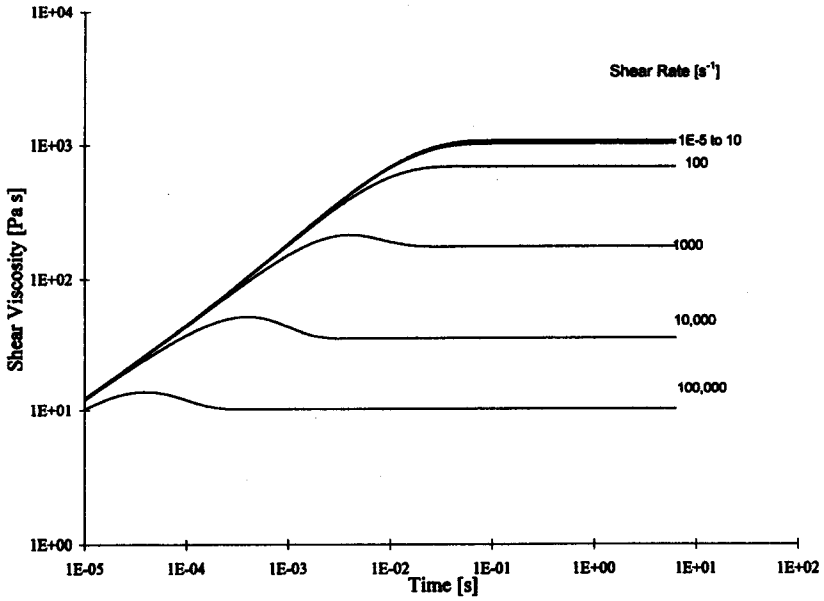

Fig. 12 Shear viscosity, $\tau_{21}/\dot{\gamma}_0$, as a function of time for a polystyrene sample with a molecular weight of 65000 g/mol. The different shear rates are shown

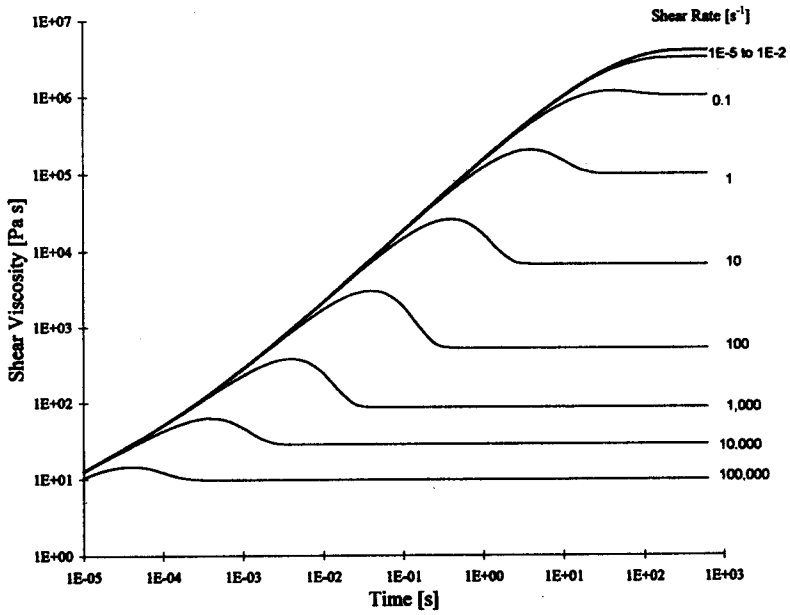

Fig. 13 Shear viscosity, $\tau_{21}/\dot{\gamma}_0$, as a function of time for a polystyrene sample with a molecular weight of 757000 g/mol. The different shear rates are shown

result is a direct consequence of the model and will be discussed later. The curves not showing stress overshoot are a consequence of the BSW spectrum only since shear thinning is still negligible. At higher rates, shear thinning sets in as predicted from the damping function, $h(t;t')$.

To get further insight, the shear viscosity as a function of the shear rate is shown in Figs. 14 and 15 for two polystyrene samples with a molecular weight of 65000 and 757000 g/mol, respectively. A surprising result of the calculations is that in the shear thinning region, the values of the viscosity predicted for long times fall below the values predicted for shorter times if the shear rate is the same. This is not an inaccuracy of the calculation, which is accurate up to the fifth significant digit; therefore, it should be taken as a prediction of the model together with Wagner's damping function.

For the sake of completeness, we present here the predicted steady shear viscosity, $\eta(\dot{\gamma}_0)$, and first normal stress difference in steady shear, $(\pi_{11}-\pi_{22})/(\dot{\gamma}_0)^2$.

$$\eta(\dot{\gamma}) = \frac{\tau_{21}}{\dot{\gamma}_0} = \int_0^{\lambda_{max}} d\lambda \frac{H(\lambda)}{(1+n_1\lambda\dot{\gamma}_0)^2} \tag{25}$$

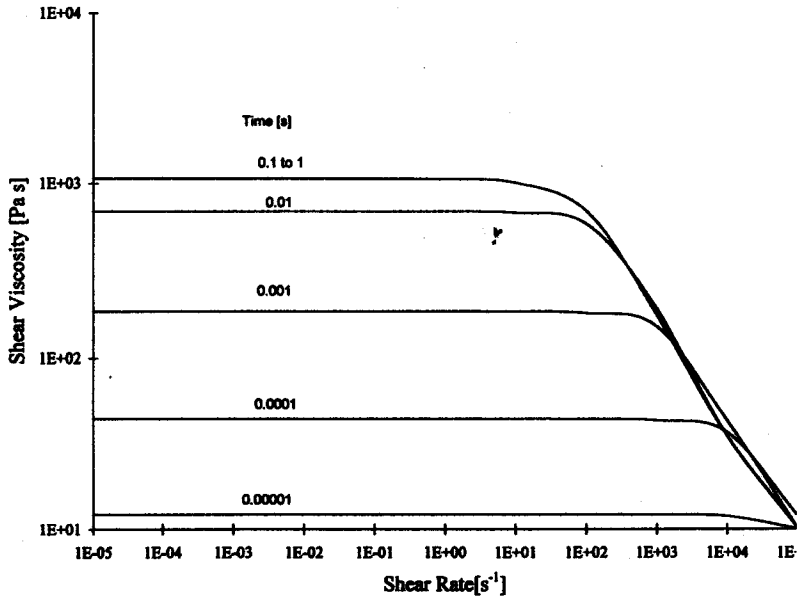

Fig. 14 Shear viscosity, $\tau_{21}/\dot{\gamma}_0$, as a function of shear rate for a polystyrene sample with a molecular weight of 65000 g/mol. The different times are shown

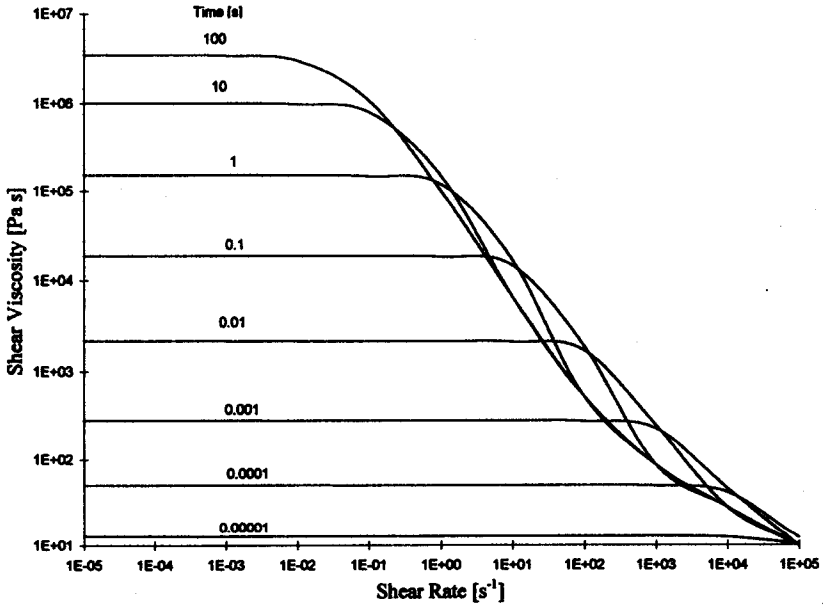

Fig. 15 Shear viscosity, $\tau_{21}/\dot{\gamma}_0$, as a function of shear rate for a polystyrene sample with a molecular weight of 757000 g/mol. The different times are shown

$$\frac{\pi_{11}-\pi_{22}}{(\dot{\gamma}_0)^2} = 2\int_0^{\lambda_{max}} d\lambda \frac{H(\lambda)\lambda}{(1+n_1\lambda\dot{\gamma}_0)^2} \tag{26}$$

Both integrals are easy to calculate and can be evaluated in terms of hypergeometric functions, but we will not pursue that calculation here.

Discussion

The empirical BSW spectrum is the most simple known form of a function which, together with Eq. (9), is able to accurately describe G', G'' data of polymers with linear flexible molecules of uniform molecular weight. A more detailed spectrum could only be proposed from theory. It could not be extracted from the experimental data due to the Morozov (1984) Discrepancy Principle which expresses the fact that a physical model for describing a data set cannot be of higher accuracy than the noise in the data.

With the exception of dynamic mechanical experiments, yielding G', G'' data, linear polymers of uniform length have been studied very little experimentally. The BSW spectrum gives us the opportunity to predict rheological material functions for a wide range of kinematics. We attempted to cover all the important ones in this paper. The calculations give a self-consistent picture.

The first important result is the retardation spectrum. This spectrum has been calculated analytically, thus no numerical integration is required for its evaluation. As expected, all the spectra fall on the same curve (slope n) for short retardation times which correspond to the glass-transition modes; these modes are short-ranged, thus independent of molecular weight. It must be mentioned that the slope of all the spectra in this region is the inverse of the slope of the relaxation spectrum. This can be proven mathematically and the result was given in Eq. (5b). It is a property of the BSW spectrum. On the other hand, long retardation times show a strong dependence on molecular weight as expected because they involve long-ranged molecular motions. Also, in the case when the retardation time is close to the maximum retardation time, the spectra drop to zero; this is because of the cut-off in the BSW relaxation spectrum. Therefore, we do not expect that these spectra can be evaluated accurately near the cut-off point. Finally, the predicted retardation spectra look very similar to the experimental ones published by Nemoto and coworkers (1972).

The next result is the analytical prediction of the relaxation modulus. Again, at short times all the curves superpose because only those modes with short relaxation times (glass-transition modes) can relax; these modes are independent of molecular weight. As soon as the long-ranged motions are activated, the molecular weight effect can be seen. As observed experimentally, the width of the rubbery plateau increases with increasing molecular weight, the plateau modulus is independent of molecular weight and the terminal zone begins when the time is of the same order of magnitude as the longest relaxation time.

In the case of the dynamic mechanical behavior, the prediction of the storage and loss moduli agrees with the results obtained by Jackson et al. (1994). Also, the qualitative behavior of the dynamic quantities agrees with the one observed experimentally. In the case of $\tan(\delta) = G''/G'$, the behavior is as expected. For example, an increase in molecular weight should decrease the fluidity of the system making it more elastic, thus, decreasing the phase lag between the excitation and the response of the system. Therefore, $\tan(\delta)$ should approach zero as observed. Also, at high frequencies, the system cannot dissipate energy efficiently, therefore, it becomes more "glass-like" and its phase lag approaches a very small value independent of molecular weight.

Sometimes the crossover of G' and G'' or the maximum of G'' has been related to the plateau modulus. One of these relations is the experimental observation of Raju et al. (1981) that states

$$\frac{G_N^0}{G''_{\max}} = 3.56$$

We decided to check this relation for two samples, polystyrene and polybutadiene. The results obtained show that the ratio is equal to 4.8 for all the molecular weights of both samples. This is in reasonable agreement with Raju's measurements.

The behavior predicted for the creep compliance is similar to the one observed experimentally where the plateau compliance is independent of molecular weight, but the width of the plateau increases with molecular weight.

As stated before, all the transient and dynamic material functions fall on a unique curve in the limits of short times and high frequencies, respectively. This is a consequence of the BSW spectrum and can be understood in the following way. At short times (high frequencies) the behavior of the material is described by the glass-transition part of the spectrum because only short-ranged correlated motions involving a few mers are active. Therefore, the value of the transient (dynamic) material functions should be independent of the molecular weight. This is captured by the BSW spectrum because the molecular weight dependence appears in the $\lambda_{\max}$ parameter which is present in the entanglement part of the spectrum.

The predictions in the non-linear viscoelastic regime agree qualitatively with what is known from experimental observations. In the case of the start-up of uniaxial extension at constant rate, the results agree with the previous results of Chang et al. (1972). In the case of the start-up of shear flow at constant rate, the BSW spectrum together with Wagner's damping function are able to predict the stress overshoot observed experimentally, the conditions when this overshoot should be observed and the time at which it should occur. Also, the model predicts the shear thinning behavior. In both experiments, the viscosity has a value independent of molecular weight at short times as explained previously.

Conclusions

The universality of the linear viscoelastic behavior of long linear flexible monodisperse polymers can be studied with the example of two polymer species, polystyrene and polybutadiene in our case. The BSW spectrum allows self-consistent predictions for the flow regime, the elastic or entanglement regime, and the glass transition. While agreement with experimental data is known

to be excellent for dynamic mechanical material functions, more data are needed for the other flow geometrics and transients.

The power law in the entanglement region seems to be a clear signature of the linear flexible chains of uniform length. Not so clear from the experiments is the crossover to the power law of the glass transition (we decided on a linear superposition) and the cut-off at the longest relaxation time. The data do not allow us to distinguish between an abrupt cut-off or a continuous but rapid drop. Our choice of an abrupt cut-off did not cause any inconsistency in the predictions from the BSW spectrum and we decided to stay with it.

Analytical expressions were found for many of the material functions which makes it easier to calculate them and compare with experiments. It also reduces the description of the material functions to a unique set of material parameters consisting of the longest relaxation time, λ_{max}, the plateau modulus, G_n^0, the slopes of the spectrum in the entanglement region (m) and in the glass transition region $(-n)$, and the crossover time, λ_c. The crossover time provides a very useful reference time; it is material specific and it encompasses the dependence of relaxation on temperature and pressure while being independent of molecular weight.

In the non-linear viscoelastic regime, the BSW spectrum has been able to capture some major effects like shear thinning, stress overshoot and the divergence of the elongational viscosity in an uniaxial extension experiment.

The results obtained show the necessity of more experiments in order to test the quantitative predictions of this work. In the future, the spectrum should be extended to polydisperse melts and solutions, branched polymers, and miscible blends.

Acknowledgement This study was supported by the Materials Research science and Engineering Center of the University of Massachusetts.

Appendix A

Hypergeometric functions arise as the solutions for the hypergeometric differential equation

$$z(1-z)\frac{d^2y(z)}{dz^2}+\{\gamma-(\alpha+\beta+1)z\}\frac{dy(z)}{dz}-\alpha\beta y(z)=0 \tag{A1}$$

The solution to this equation can be written down in the form of a Taylor expansion if the argument, z, is in the interval $(-1, 1)$ and the coefficients satisfy that $\gamma-(\alpha+\beta)>-1$. The first terms of the series are shown in Eq. (A2).

$$F(\alpha,\beta;\gamma;z)=1+\frac{\alpha\beta}{1\cdot\gamma}z+\frac{\alpha(\alpha+1)\beta(\beta+1)}{1\cdot2\cdot\gamma(\gamma+1)}z^2+\frac{\alpha(\alpha+1)(\alpha+2)\beta(\beta+1)(\beta+2)}{1\cdot2\cdot3\cdot\gamma(\gamma+1)(\gamma+2)}z^3+\ldots \tag{A2}$$

The solution can be expressed in an integral form, Eq. (A3). It was this expression that appeared in our calculations and led to the appearance of this type of functions in our analysis.

$$F(\alpha,\beta;\gamma;z)=\frac{\Gamma(\gamma)}{\Gamma(\beta)\Gamma(\gamma-\beta)}\int_0^1 u^{\beta-1}(1-u)^{\gamma-\beta-1}(1-uz)^{-\alpha}du \tag{A3}$$

Finally, many times it was necessary to evaluate this function for arguments larger than unity for which the series does not converge. For this case, we have used the analytic continuation of the function shown in Eq. (A4).

$$F(\alpha,\beta;\gamma;z)=\frac{\Gamma(\gamma)\Gamma(\beta-\alpha)}{\Gamma(\beta)\Gamma(\gamma-\alpha)}(-1)^{\alpha}z^{-\alpha}F\left(\alpha,\alpha+1-\gamma;\alpha+1-\beta;\frac{1}{z}\right)+\frac{\Gamma(\gamma)\Gamma(\alpha-\beta)}{\Gamma(\alpha)\Gamma(\gamma-\beta)}(-1)^{\beta}z^{-\beta}F\left(\beta,\beta+1-\gamma;\beta+1-\alpha;\frac{1}{z}\right) \tag{A4}$$

Appendix B

The incomplete gamma function is a generalization of the well known gamma function.

$$\Gamma(\alpha)=\int_0^\infty e^{-t}t^{\alpha-1}dt \tag{B1}$$

The difference arises from the lower limit of integration in the integral definition of the incomplete gamma function.

$$\Gamma(\alpha,x)=\int_x^\infty e^{-t}t^{\alpha-1}dt \tag{B2}$$

The incomplete gamma function has the series representation.

$$\Gamma(\alpha,x)=\Gamma(\alpha)-\sum_{n=0}^{\infty}\frac{(-1)^n x^{\alpha+n}}{n!(\alpha+n)} \tag{B3}$$

where $\Gamma(\alpha)$ is the gamma function of argument α. Omitted are the α-values of 0, −1, −2, etc. This representation has been used in our work to calculate the value of the function.

References

Baumgaertel M, Schausberger A, Winter HH (1990) The relaxation of polymers with linear flexible chains of uniform length. Rheol Acta 29:400–408

Baumgaertel M, de Rosa ME, Machado J, Masse M, Winter HH (1992) The relaxation time spectrum of nearly monodisperse polybutadiene melts. Rheol Acta 31:75–82

Bird RB, Armstrong RC, Hassager O (1987) Dynamics of polymeric liquids, vol 1. John Wiley and Sons, New York

Chang H, Lodge AS (1972) Comparison of rubberlike-liquid theory with stress-growth data for elongation of a low-density branched polyethylene melt. Rheol Acta 11:127–129

de Gennes P (1979) Scaling concepts in polymer physics. Cornell University Press, Ithaca

des Cloizeaux J (1990) Relaxation and viscosity anomaly of melts made of long entangled polymers. Time-dependent reptation. Macromolecules 23:4678

Doi M, Edwards SF (1986) The theory of polymer dynamics. Clarendon Press, Oxford

Ferry JD (1980) Viscoelastic properties of polymers, 3rd ed. John Wiley and Sons, New York

Gradshteyn IS, Ryzhik IM (1980) Table of integrals, series and products, 4th ed. Academic Press, London

Graessley WW (1974) The entanglement concept in rheology. Adv Polym Sci 16. Springer, Heidelberg

Gross B (1953) Mathematical structure of the theories of viscoelasticity. Hermann, Paris

Jackson JK, de Rosa ME, Winter HH (1994) Molecular weight dependence of relaxation time spectra for the entanglement and flow behavior of monodisperse linear flexible polymers. Macromolecules 27:2426–2431

Knoff WF, Hopkins IL, Tobolsky AV (1971) Studies on the stress relaxation of polystyrenes in the rubbery flow region. II. Macromolecules 4:750–754

Laun HM (1978) Description of the non-linear shear behavior of a low density polyethylene melt by means of an experimentally determined strain dependent memory function. Rheol Acta 17:1–15

Lodge AS (1964) Elastic liquids. Academic Press, New York

Marin G, Graessley WW (1977) Viscoelastic properties of high molecular weight polymers in the molten state: I – Study of narrow molecular weight distribution samples. Rheol Acta 16:527

Meissner J (1971) Dehnungsverhalten von Polyäthylen-Schmelzen. Rheol Acta 10:230–242

Morozov V (1984) Methods for solving incorrectly posed problems. Springer, Berlin

Nemoto N, Odani H, Kurata M (1972) Shear creep studies of narrow-distribution poly-(cis-isoprene). II. Extension to low molecular weights. Macromolecules 5:531–535

Onogi S, Masuda T, Kitigawa K (1970) Rheological properties of anionic polystyrenes. I. Dynamic viscoelasticity of narrow-distribution polystyrenes. Macromolecules 3:109–115

Osaki K (1976) Nonlinear viscoelasticity of polymer solutions. Proc 7th Intl Congr on Rheology, Gothenburg, pp 104–109

Papanastasiou AC, Scriven LE, Macosko CW (1983) An integral constitutive equation for mixed flows: Viscoelastic characterization. J Rheol 27:387–410

Raju VR, Menezes EV, Marin G, Graessley WW, Fetters LJ (1981) Concentration and molecular weight dependence of viscoelastic properties in linear and star polymers. Macromolecules 14:1668–1676

Rouse PE (1953) A theory of linear viscoelastic properties of dilute solutions of coiling polymers. J Chem Phys 21:1272–1280

Schausberger A, Schindlauer G, Janeschitz-Kriegl H (1985) Linear elastic-viscous properties of molten standard polystyrenes. I. Presentation of complex moduli; role of short range structural parameters. Rheol Acta 24:220

Schweizer KS, Szamel G (1995) Transport theory and statistical physics 24:947

Soskey PR, Winter HH (1984) Large step shear strain experiments with parallel-disk rotational rheometers. J Rheol 28:625–645

Tobolsky AV (1960) Properties and structures of polymers. John Wiley and Sons, New York

Wagner MH (1976) Analysis of time-dependent non-linear stress-growth data for shear and elongational flow of a low-density branched polyethylene melt. Rheol Acta 15:136–142

Wagner MH (1978) A constitutive analysis of uniaxial elongation flow data of a low-density polyethylene melt. J Non-Newtonian Fluid Mech 4:39–55